Proceedings of the 7th International Conference on Mechanics and Materials in Design
Albufeira/Portugal 11-15 June 2017. Editors J.F. Silva Gomes and S.A. Meguid.
Publ. INEGI/FEUP (2017)

PAPER REF: 6460

NEW TECHNOLOGY FOR INVESTMENT CASTING CERAMIC MOULD MANUFACTURE WITH A CERAMIC FIBERS MATERIALS NEW GENERATION

Rafal Cygan(*)
Faculty of Mechanical Engineering and Aeronautics, Rzeszow University of Technology, al. Powstancow Warszawy 8, Rzeszow 35-959, Poland
(*)*Email:* rafal.cygan@cppcorp.com

ABSTRACT

Most of the critical components responsible for safe operation of the aircraft engine are made of heat resistant nickel-based superalloys. The main manufacturing process, that is used for aircraft engine hot section components, is investment casting technology, which is based on use of multilayer ceramic moulds. The use of modern ceramic materials containing fibers will improve technological parameters of the ceramic moulds.

Keywords: ceramic moulds, fibres, investment casting, aerospace.

INTRODUCTION

Cost reduction in production by investment casting method is associated with reduction in the "poor quality" cost which is one of the basic problems in the foundry industry. Reducing this costs is associated with optimization of manufacturing technology of aircraft engine critical elements and can be achieved by improving properties of self-supporting ceramic moulds.

Important technological problem in production of castings from nickel-based superalloys is to develop manufacturing technology for ceramic moulds with assumed technological parameters. Improvement of these parameters can be achieved through use of a new generation of ceramic materials [1-3].

The problem of defects in castings despite the use of advanced techniques is not yet resolved [4]. There is a lack of comprehensive design and evaluation of the impact on the ceramic mould during annealing, casting and solidification process in the area of thin-walled castings, as it is in case of trailing edge of the blades. It does not allow to determine the definite causes of defects appearance. This is due to limited, by global foundries producing elements of aircraft engine hot sections, available technological expert knowledge. In many foundries there is a need to resolve these issues linked with change of both types of castings and introduction of new ceramic materials [5-7].

Test results allow accurate determination of the impact of applied type of ceramics and fibers on improvement of technological properties as permeability and strength of the ceramic mould during annealing process and the initial pouring and solidification. These data are necessary to determine the impact of geometrical characteristic change on temperature distribution in the mould. Thus also on the orientation of the solidification front during the manufacturing process. Obtained knowledge will significantly contribute to reduce the

workload and thus the cost of production, not only in the aircraft industry, but also in meaning of castings of machine components manufactured by investment casting method [8-12].

RESULTS AND CONCLUSIONS

The test materials are 3 moulding binders. Below, basic properties of tested adhesives are presented, that were specified by the manufacturer [4].

The first binder (market as 1) is an aqueous colloidal suspension containing alkaline silica of approx. 30% by weight. The silica sol is stabilized by addition of sodium. The particles have negative surface charge, a spherical shape and are of similar sizes. The binder 1 has form of a semi-transparent liquid with a viscosity slightly in excess of water.

The binders 2 and 3 are acrylic emulsion polymers, of white colour and a solid content of 48-50%. Additionally, binder 3 consists of vitreous fibres of 1-10% by weight.

Table1. Chemical composition of investigated binders (by the producer) [5]

Binder	Compound	Content [mass %]
1	Silica (amorphous)	20-40
2	Non-ionic alcohol (surfactant)	1-10
	Acrylic polymer emulsion	80-95
	Ammonia	<0,1
	2,2’2”(heksahydro-1,3,5-triazyno-1,3,5 tryil) trietanol	2
	Diphenyl ketone	0.3
3	Non-ionic alcohol (surfactant)	1-10
	Acrylic polymer emulsion	80-95
	Ammonia	0.1
	2,2’2”(heksahydro-1,3,5-triazyno-1,3,5 tryil) trietanol	2
	Synthetic vitreous fibres	1-10

Figure 1 presents the results of microstructure investigation of binder 1, which was carried out using STEM technique. On the basis of the investigation, it was found that the tested binder contains SiO_2 particles of spherical shape. Observed particles have a diameter of approx. 5 to 20 nm and are clustered in agglomerates with sizes ranging from 100 nm to several microns.

Figure 2 and table 2 present the results of particles and agglomerates size measurements carried out using DLS technique. The resulting particle size distribution consists of three peaks - most intense corresponding to the particle equivalent diameter of approx. 200 nm and two peaks with lower intensities, corresponding to particles with a diameter equivalent to approx. 5 nm and approx. 4.2 μm. The results correspond to STEM observations (Fig. 1). Less intense peak for the size of approx. 5 nm corresponds to spherical particles of SiO2, while peaks obtained for the size of approx. 200 nm and approx. 4.2 microns suit their agglomerates.

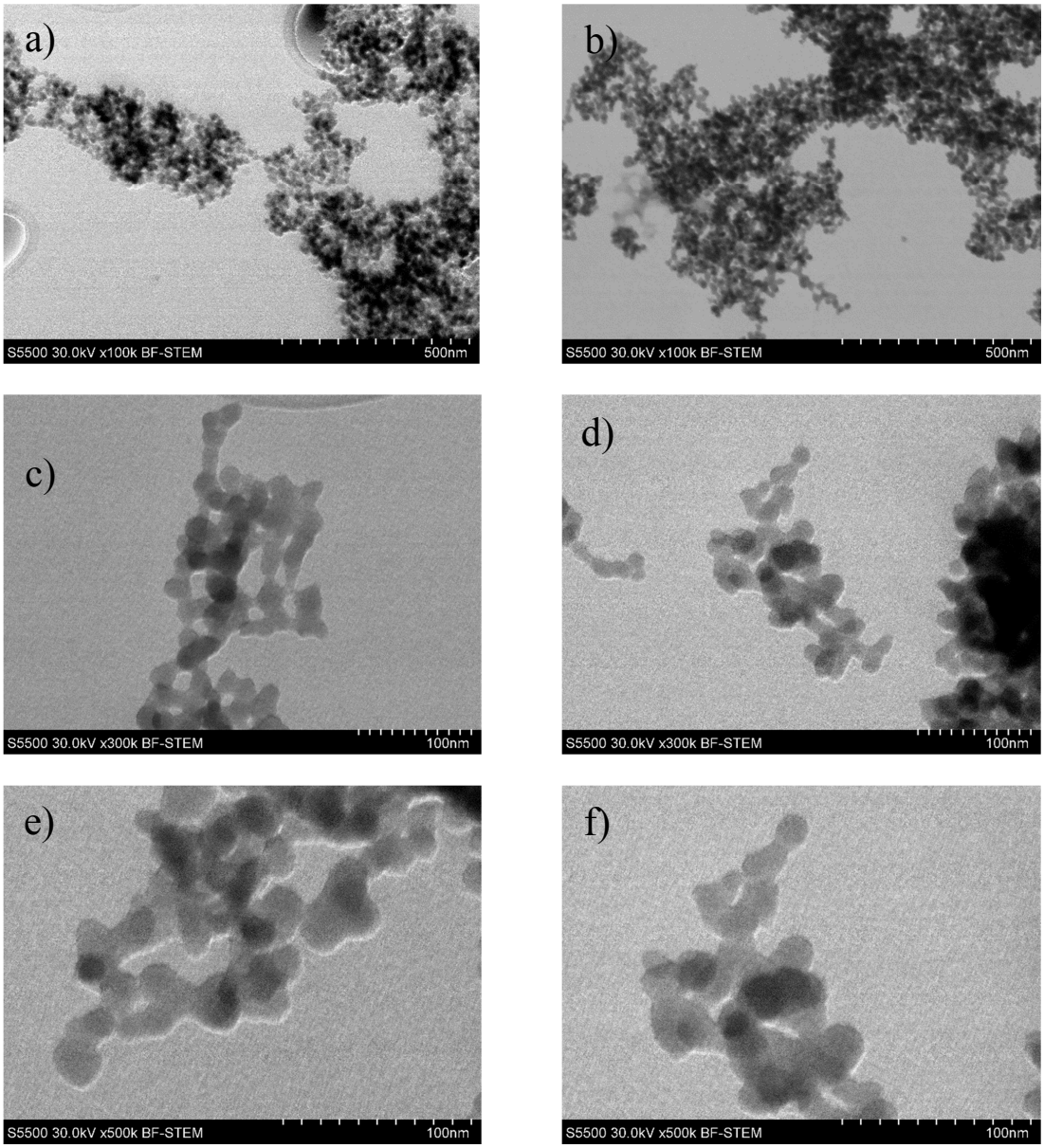

Fig. 1 - Microstructure of binder 1

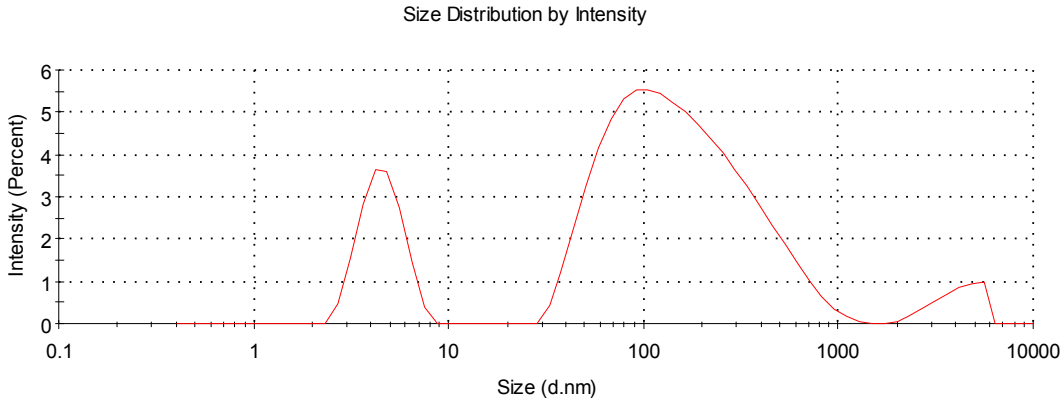

Fig. 2 - Particle size distribution for binder 1

Table 2 - Equivalent diameters of particles and intensity of the peaks for binder 1

	Diameter d [nm]	Intensity [%]
peak 1	198	79
peak 2	5	17
peak 3	4187	5

Figure 3 and table 3 show the results of DLS analysis performed on binder 1 after the process of breaking the agglomerates in an ultrasound bath for 15 min. The resulting particle size distribution consists of three peaks - corresponding to the most intense particle equivalent diameter of approx. 130 nm and two peaks with lower intensities, corresponding to particles with a diameter equivalent to approx. 5 nm and approx. 2.5 μm. Obtained results indicate reduction in the size of the agglomerates from approx. 200 nm and 4.2 microns to approx. 130 nm and 2.5 microns after treatment in an ultrasound bath. The size of individual SiO_2 particles has not changed and is approx. 5 nm.

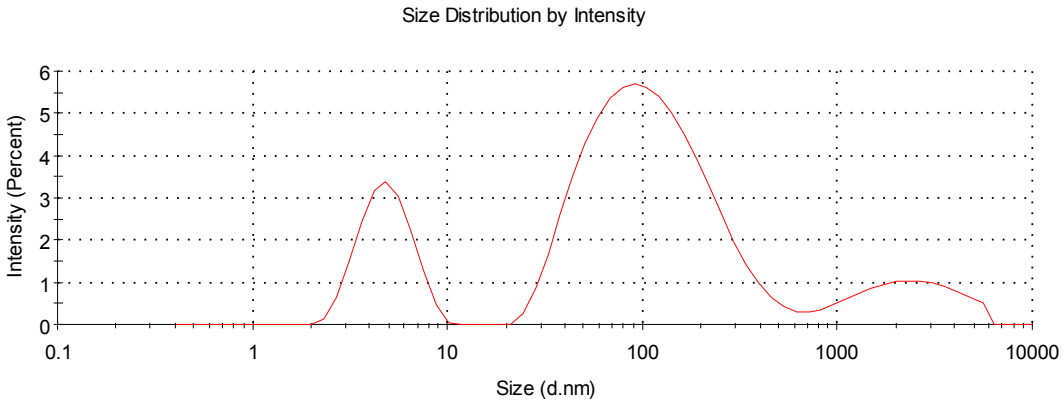

Fig. 3 - Particle size distribution in binder 1 after breaking by ultrasonication for 15 min

Table 3 - Equivalent diameters of particles and intensity of the peaks of binder 1 broken by ultrasonication for 15 min

	Diameter d [nm]	Intensity [%]
peak 1	132	71
peak 2	5	18
peak 3	2511	11

Figure 4 presents TGA analysis results for binder 1. Differential thermogravimetric curve shows peak corresponding to maximum temperature of approx. 63 °C. Mass decrease at such low temperature is caused by evaporation of the water bound in the binder. The mass remaining after pyrolysis of approx. 94% of the original mass of the sample corresponds to the silica.

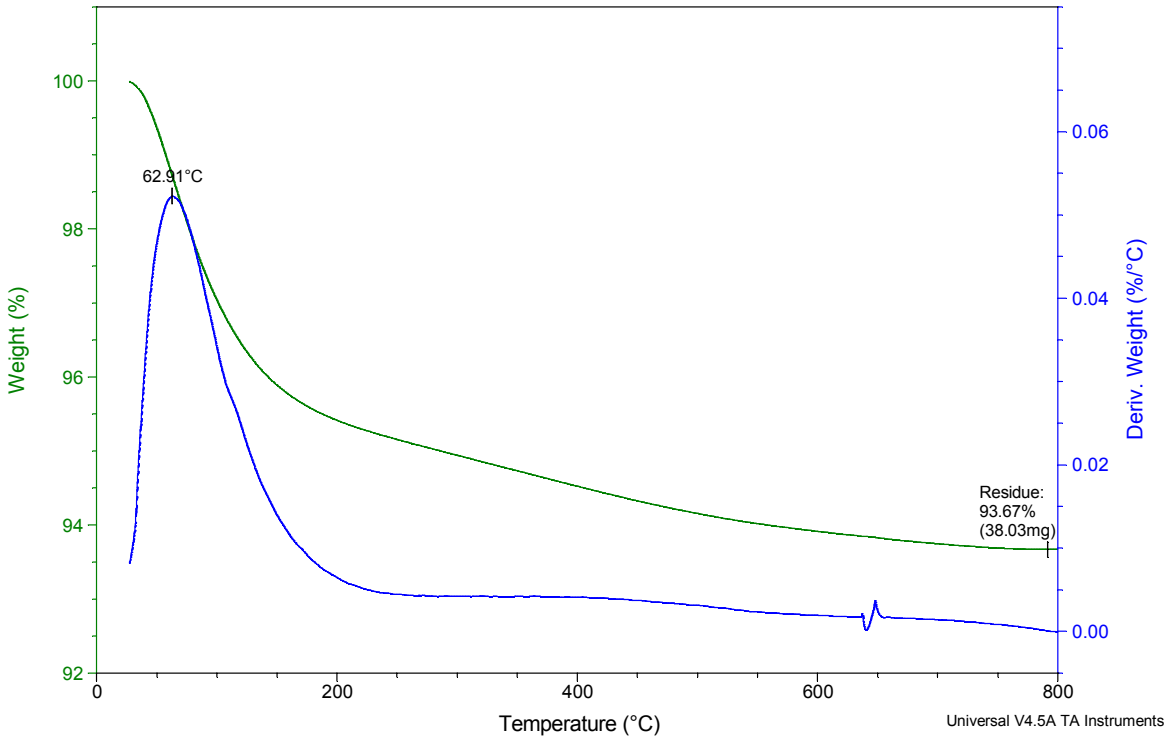

Fig. 4 - TGA analysis results for binder 1

Figure 5 presents the results of particle size measurements for binder 2, which was carried out using DLS technique. Resulting distribution of particles shows one peak corresponding to a maximum equivalent diameter of particles of 173 nm. Figure 6 shows the results of DLS analysis performed for binder 2 after the process of breaking the agglomerates in an ultrasound bath for 15 min. Resulting particle size distribution also has a peak corresponding to the equivalent particle diameter of 173 nm. Based on the results, it was found that the polymer particles contained in the binder are unagglomerated and have a size of approx. 170 nm.

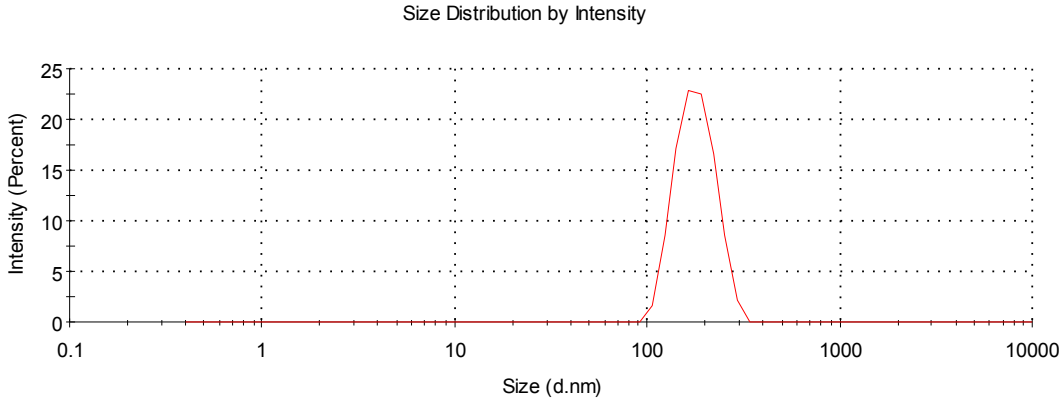

Fig. 5. Particle size distribution in binder 2

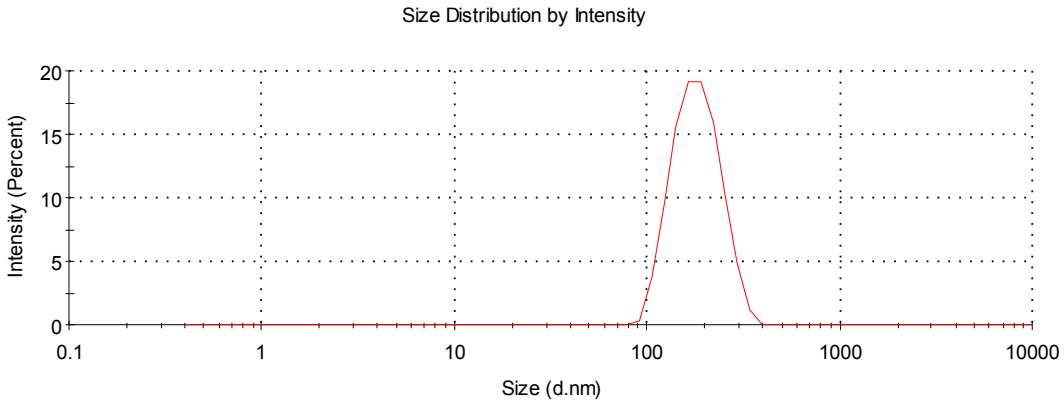

Fig. 6 - Particle size distribution in binder 2 after breaking by ultrasonication for 15 min

Figure 7 presents TGA analysis results for binder 2. Differential thermogravimetric curve shows two peaks with maximum values of 117 °C i 396 °C. First of them corresponds to the first stage of decomposition characterized by mass loss on the level of 7.8%. This peak can be identified as a result of loss of water, alcohol, or 2,2'2 "(hexahydro-1,3,5-triazine-1,3,5 tryil) triethanol present in the binder. The second peak corresponds to polymer decomposition, where the mass loss is on the level of approx. 86.8%. The remains of the pyrolysis process are approx. 5.3% of the original mass.

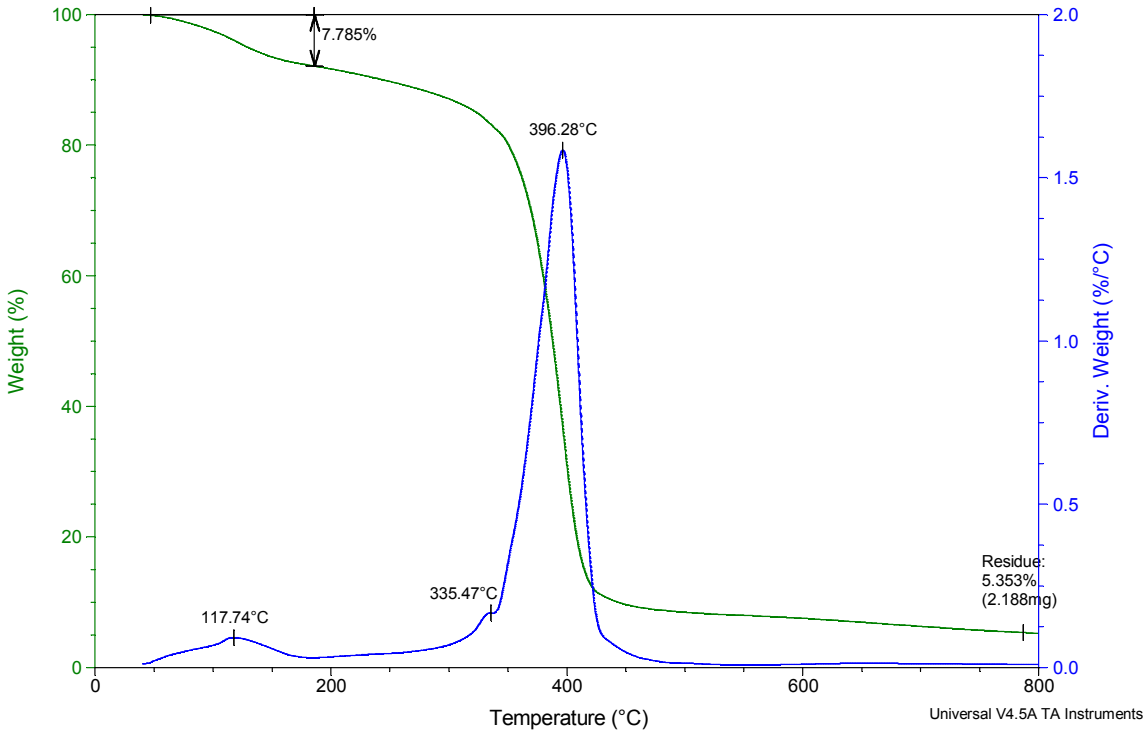

Fig. 7 - TGA analysis results for binder 2.

Figure 8 presents the results of particle size measurements for binder 3, which were carried out using DLS technique. As with the binder 2, obtained particle size distribution shows only one peak. The maximum values corresponds to equivalent diameter of the particles on the level of 169 nm., Figure 9 and showed the results of DLS analysis performed on investigated binder after the process of breaking the agglomerates in an ultrasound bath for 15 min.

Resulting particle size distribution also has a peak corresponding to the equivalent particle diameter of 161 nm. Based on obtained results it was concluded that that the polymer particles contained in the binder have uniform size of approx. 160-169 nm and are not agglomerated.

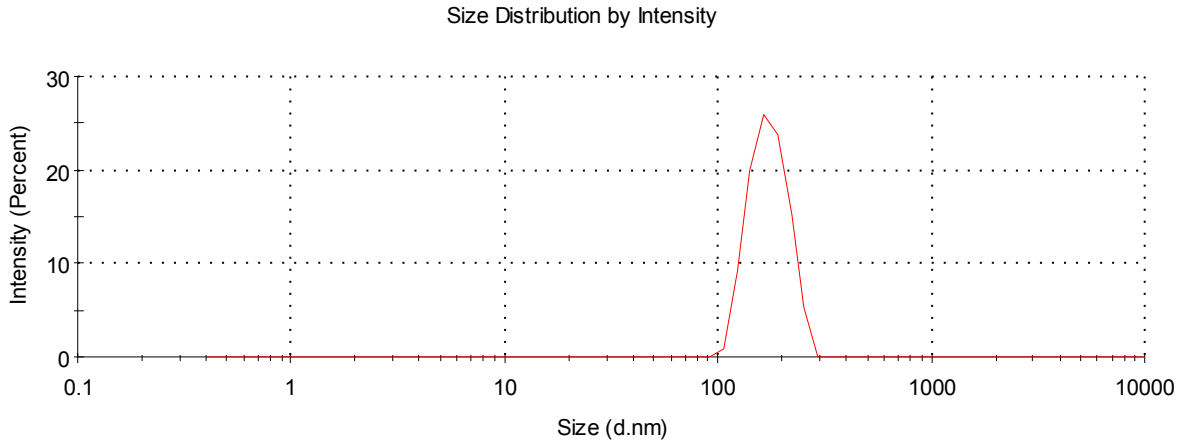

Fig. 8 - Particle size distribution in binder 3

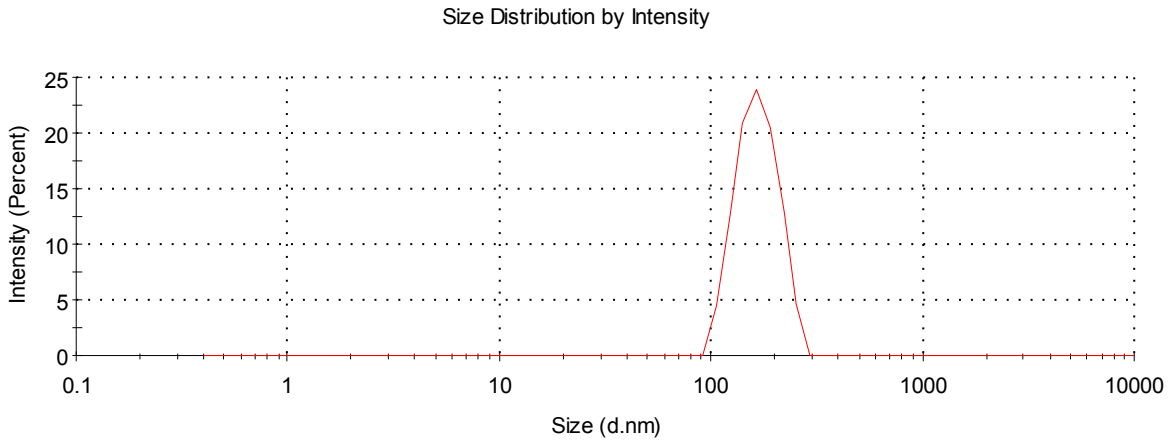

Fig. 9 - Particle size distribution in binder 3 after breaking by ultrasonication for 15 min

Figure 10 Residues after pyrolysis of the binder Based on these results, it was found that the mass remaining after the pyrolysis process corresponds to the fibers used in the binder 3.

Figure 11 presents TGA analysis results for binder 3. Differential thermogravimetric curve shows peak corresponding to maximum temperature of 397 °C. It is linked to polymer decomposition with mass loss on the level of 90%. The remains of the pyrolysis process are approx. 10% of the original mass.

Fig. 10 - Residues after pyrolysis of the binder 3

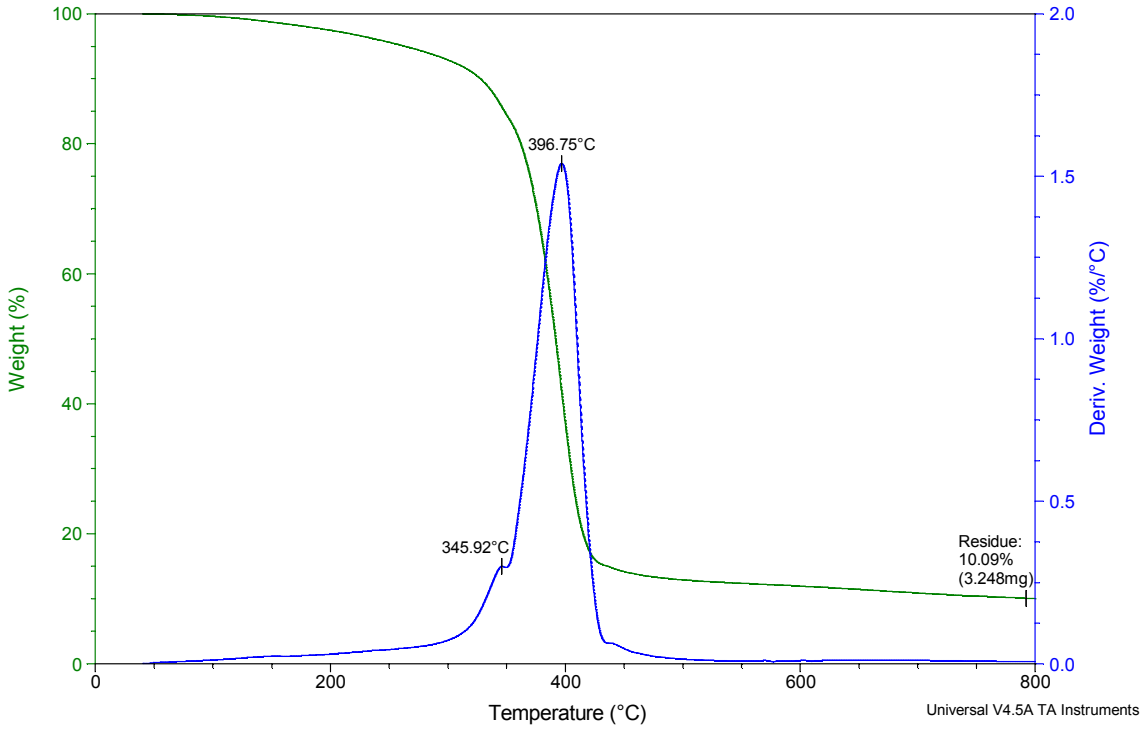

Fig. 11 - TGA analysis results for binder 3

In order to investigate chemical and phase composition, the fibers were separated from the binder 3 submitted to multi step filtration through a sieve and then washed. Separated fibers are presented in figure 12. They are of a white colour and a length up to 10 mm.

Fig. 12 - Fibers separated from the binder 3

Figure 13 shows separated fibers by meaning of light microscopy. They are transparent of a thickness of approx. 5-10 mm.

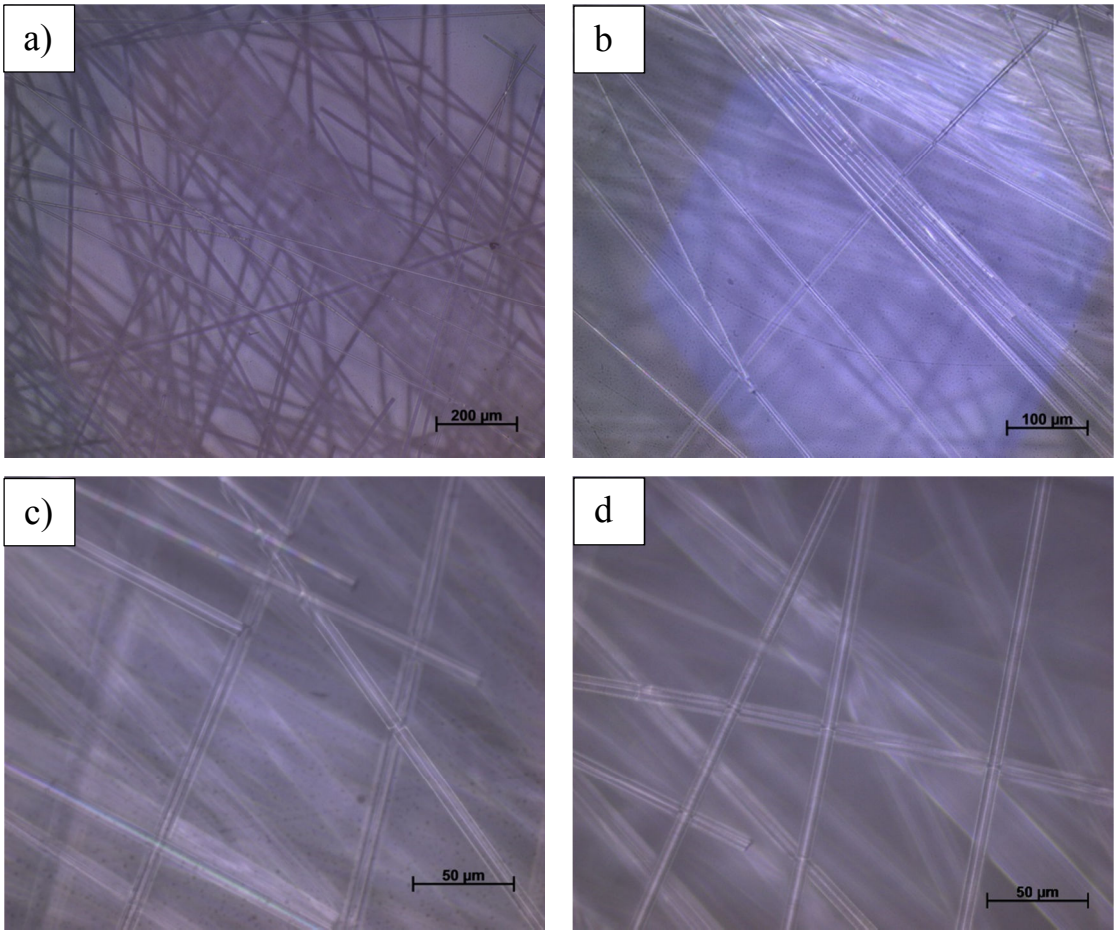

Fig. 13 - Fibbers separated from the binder 3 - light microscopy

Figures 14 and 15 present SEM and EDS analysis results of investigate fibers. Based on the results it was found, that investigated fibers consist mainly calcium. The other detected elements are silicon and aluminium. Investigated chemical composition corresponds to composition of glass fibres.

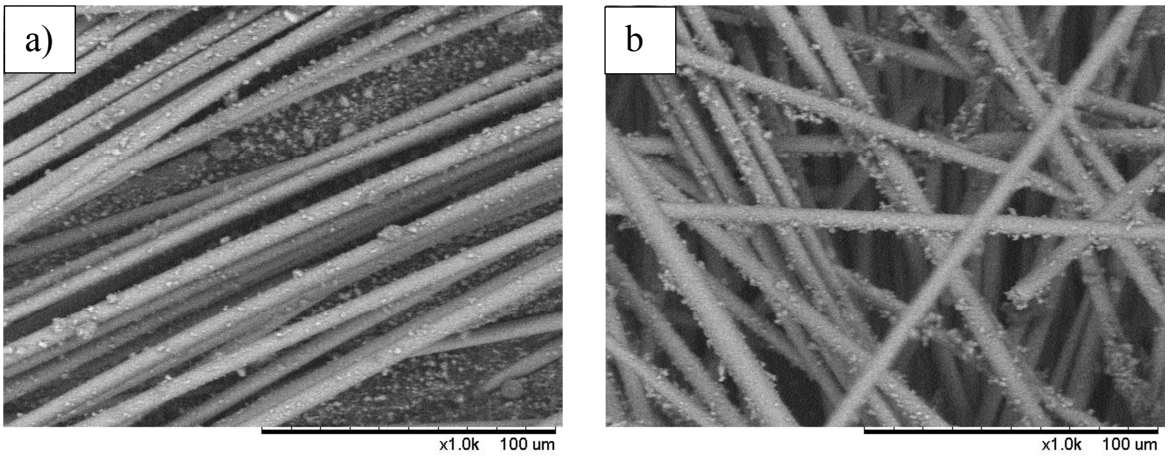

Fig. 14 - Fibers separated from the binder 3 - SEM

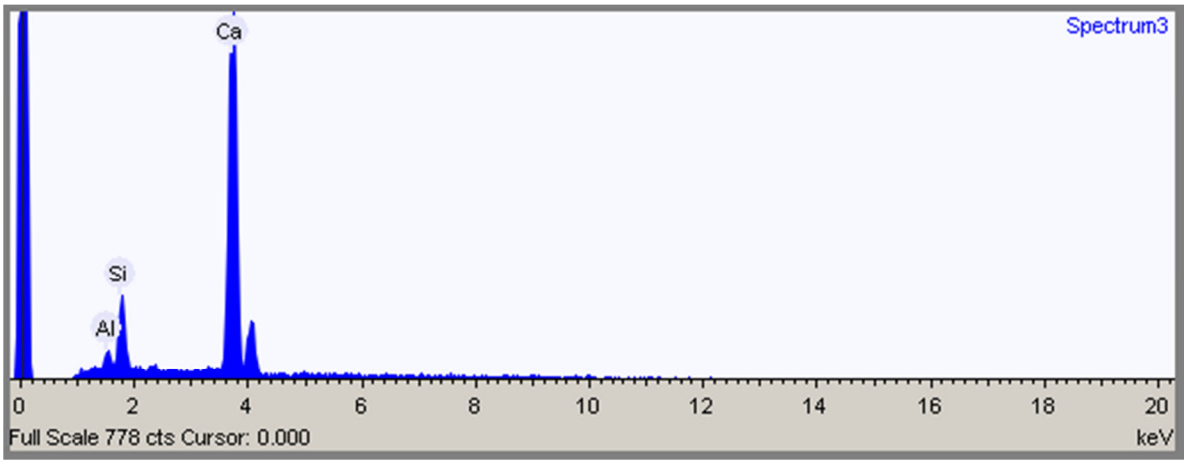

Fig. 15 - Fibers separated from the binder 3 - EDS spectrum

Table 4 - Fibers separated from the binder 3 - EDS spectrum

Element	mass %
Al	3
Si	10
Ca	88

CONCLUSION

The study involved two types of binders - one containing silica particles with a size of approx. 5 nm present in the agglomerates of 200 nm and 4 microns, and binders 2 and 3 containing particles of polymethacrylate and polyacrylamide butyl of approx. 170 nm size. Binder 1 shows lower viscosity by three orders of magnitude compared to binders 2 and 3. All tested binders are stable at pH above 6. Additionally binder 3 consists of calcium aluminate glasses (CAG). The addition of them in the moulding binder results in composite mould with enhanced strength. The differences in thermal expansion coefficients of the fibers and the mould and the phenomenon of glass fibers solidification [9]may increase porosity and gas permeability in the moulds.

ACKNOWLEDGMENTS

The authors gratefully acknowledge the funding by National Centre for Research and Development Poland, under grants LIDER Nr LIDER/227/L-6/14/NCBR/2015 “New technology for investment casting manufacturing critical components engine with a ceramic materials new generation”.

REFERENCES

REFERENCES

[1]-ASM Handbook Volume 15: Casting. ASM International, 1992.

[2]-R. Haratym, R. Biernacki, and D. Myszka, Ekologiczne wytwarzanie dokładnych odlewów w formach ceramicznych. Oficyna Wydawnicza Politechniki Warszawskiej, 2008.

[3]-J. A. Rodríguez and M. Fernández-García, Eds., Synthesis, Properties, and Applications of Oxide Nanomaterials. Hoboken, NJ, USA: John Wiley & Sons, Inc., 2007.

[4]-Hubert Matysiak, Malgorzata Zagorska, Alicja Balkowiec, Boguslawa Adamczyk-Cieslak, Krzysztof Dobkowski, Mateusz Koralnik, Rafal Cygan, Jacek Nawrocki, Jan Cwajna, Krzysztof J Kurzydlowski, The Influence of the Melt-Pouring Temperature and Inoculant Content on the Macro and Microstructure of the IN713C Ni-Based Superalloy, JOM: the journal of the Minerals, Metals & Materials Society, 2015/10, p 1-13.

[5]-“Ransom & Randolph.” [Online]. Available: http://www.ransom-randolph.com/.

[6]-P. R. Foy, “Fabrication and characterization of calcium aluminate glass fibers,” J. Nanosci. Nanotechnol., vol. 8, no. 10, pp. 5166-5171, 2008.

[7]-Y. Wang, C. Zu, K. He, H. Zhao, B. Han, and J. Chen, “Crystallization kinetics of calcium aluminate glasses studied by non-isothermal techniques,” J. Wuhan Univ. Technol. Mater. Sci. Ed., vol. 28, no. 5, pp. 907-911, 2013.

[8]-Magdalena Gromada, Adam Świeca, Marek Kostecki, Andrzej Olszyna, Rafał Cygan, Ceramic cores for turbine blades via injection moulding, Journal of Materials Processing Technology, 2015/6/30, 220, p 107-112

[9]-M. V. Zasolotskaya, K. A. Dobrovol'skii, V. E. Khazanov, and V. N. Zueva, "Relationship between crystallization and shrinkage in superfine quartz fibers and their impurities," Glas. Ceram., vol. 45, no. 1, pp. 23-26, Jan. 1988.

[10]-H. Matysiak, M. Zagorska, J. Andersson, A. Balkowiec, R. Cygan, M. Rasinski, M. Pisarek, M. Andrzejczuk, K. Kubiak, and K.J. Kurzydlowski, Microstructure of Haynes® 282 ® Superalloy After Vacuum Induction Melting and Investment Casting of Thin-Walled Components, Materials, 2013, 6, p 5016-5037

[11]-S. Roskosz, D. Szeliga, R. Cygan, P. Rokicki, Investment casting design and processing for drone's micro-engine turbone rotor manufactuing, Solid State Phenomena Col 246, 2016, p 189-192

[12]-A. Nowotnik, P. Rokicki, G. Mrówka-Nowotnik, J. Sieniawski, Dynamic Precipitation of Nickel-Based Superalloys Undergoing Severe Deformation Below the Solvus Temperature, International Journal of Materials Research 106 (7), 2015, p 665-675.